PHILOSOPHICAL TRANSACTIONS OF THE ROYAL SOCIETY A MATHEMATICAL, PHYSICAL & ENGINEERING SCIENCES

Thermal Regime of the Northern Bay of Biscay Continental Margin in the Vicinity of the D.S.D.P. Sites 400-402

J.-P. Foucher and J. C. Sibuet

Phil. Trans. R. Soc. Lond. A 1980 **294**, 157-167
doi: 10.1098/rsta.1980.0022

Phil. Trans. R. Soc. Lond. A **294**, 157–167 (1980) [157]
Printed in Great Britain

Thermal régime of the northern Bay of Biscay continental margin in the vicinity of the D.S.D.P. Sites 400–402†

By J.-P. Foucher and J. C. Sibuet
Centre Océanologique de Bretagne, B.P. 337, 29273 *Brest, France*

Average heat flow values on land in western Europe are about 2 h.f.u., whereas recently acquired surface-ship measurements and the downhole heat flow determinations at D.S.D.P. Site 402 indicate that the heat flow is only about one-half of this value over the continental slope and rise of the adjacent northern Bay of Biscay margin in the vicinity of the D.S.D.P. Sites 400–402. Assuming that both the margin and the adjacent continental area are close to steady state thermal conditions, we suggest that the observed heat flow contrast reflects different radioactive crustal contributions to the surface heat flow in the two areas. Under the margin, the crust is thinner and would have a smaller radioactive contribution, the decrease in the contribution being related to the nature of the crustal thinning process under the margin.

The heat flow data are compatible with a model of crustal thinning that considers this to be mainly a result of mechanical deformation of the crust through extension.

Introduction

Ten conventional oceanic surface heat flow measurements were made over the northern margin of the Bay of Biscay in the vicinity of the D.S.D.P. sites 400–402 during the RV Suroit–SU 01 (December 1975) and RV Jean Charcot–CH 66 (February 1976) cruises of C.N.E.X.O. These measurements, complemented by the heat flow determination made at Site 402 during Leg 48 of the Deep Sea Drilling Project (Erickson *et al.* 1979) provide information on the thermal régime of the margin. The main observation is that the regional heat flow over the margin is substantially lower than over the adjacent Western European continental area. We suggest in this report that the observed heat flux contrast provides constraints on the debatable nature of the crustal thinning processes under the margin.

Regional setting

The study area lies north of the Bay of Biscay over the Western Approaches margin, in the vicinity of the D.S.D.P. Sites 400–402 (figure 1). Extensive geological and geophysical work (e.g. Auffret *et al.*, Montadert *et al.*, Avedik & Howard, all 1979) as well as drilling results have provided detailed information on the structure of the margin. Under a thin upper Cretaceous to Cainozoic sediment cover of 1–2 km thickness, a series of tilted fault blocks extends from the mid-continental slope to the abyssal plain down to the Trevelyan Escarpment at a depth of about 4 km (figure 2). The fault blocks trend subparallel to the margin controlling the relief of the Meriadzek Terrace and are bounded by listric faults that become near horizontal at a depth of about 4–5 km below the sediment surface (Montadert *et al.* 1979). They consist of Mesozoic sediments drilled at Site 401, and/or Hercynian basement rocks

† Contribution no. 654 of the Scientific Department of the Centre Océanologique de Bretagne.

dredged at the base of Goban Spur at about 4 km depth (Pautot *et al.* 1976). It is now widely agreed that the fault block structure of the margin was mainly shaped during the rifting episode that is dated as Late Jurassic – Early Cretaceous and preceded the onset of the opening of the Bay of Biscay in the Upper Aptian. Structural interpretation and geophysical results suggest that the continental oceanic crust boundary lies south of the Trevelyan Escarpment (figure 1) (Montadert *et al.*, Avedik & Howard, both 1979). Under Trevelyan seismic refraction data indicate that the Moho lies at a depth of 12–13 km compared with 27–30 km under the continental shelf (Avedik & Howard 1979), implying a considerable thinning of the original continental crust.

Six of the ten surface heat flux measurements reported here form a transect from the mid-

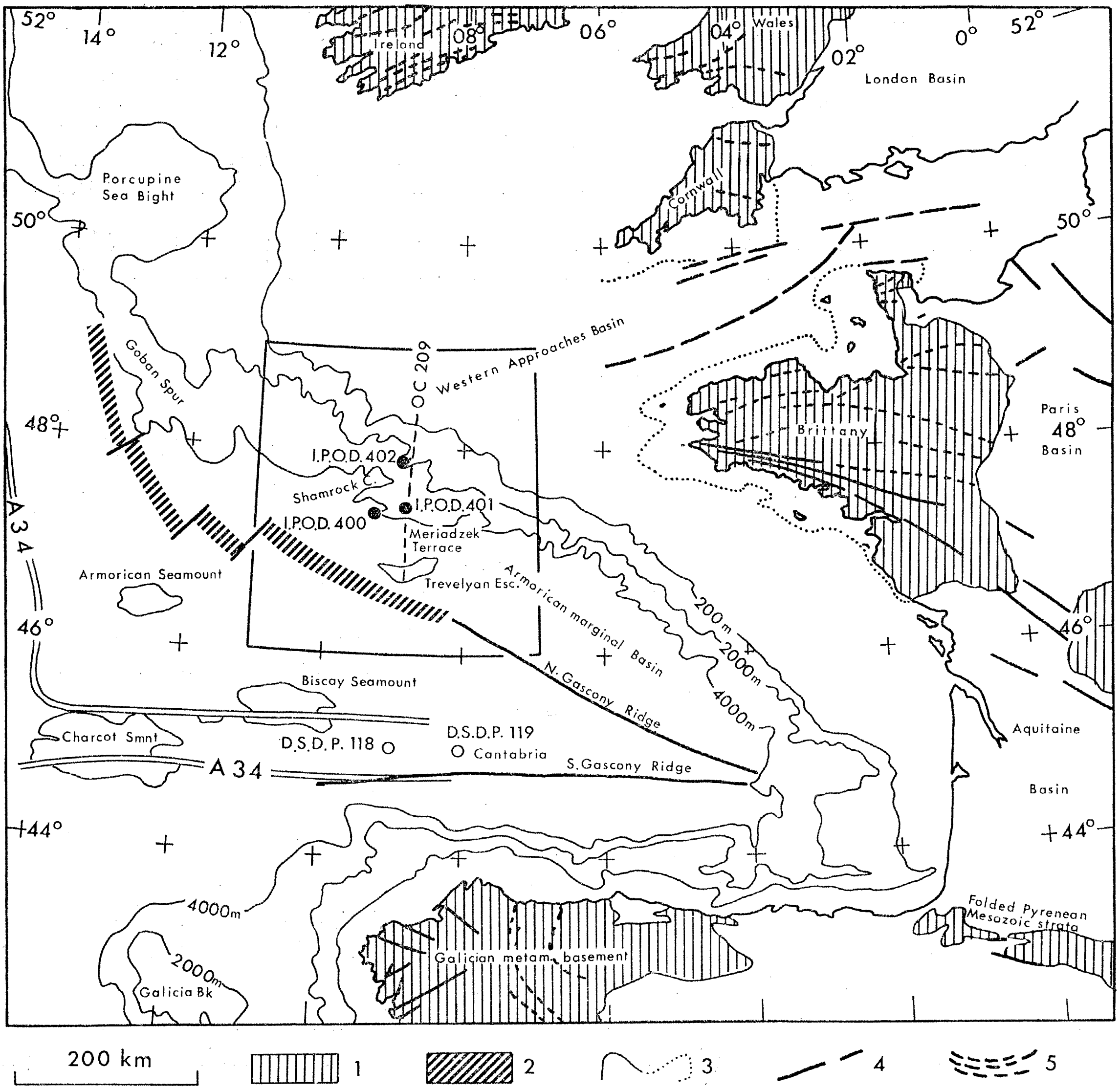

FIGURE 1. Main physiographic features of Western Europe and of the Bay of Biscay after Montadert *et al.* (1979). Magnetic anomaly 34 after Sibuet *et al.* (this volume). The hatched area shows the continental – oceanic crust boundary (Montadert *et al.* 1979). (1) Hercynian ranges and Palaeozoic basins. (2) Continent–ocean boundary (Montadert *et al.* 1979). (3) Boundaries of inshore basins. Blank areas inland represent the Mesozoic and Cainozoic basins. (4) Main fractured zones and faults. (5) Main Hercynian fold trends.

continental slope to the abyssal plain across the Meriadzek Trevelyan area; the four other measurements are located over the North Western termination of the Meriadzek Terrace known as the Aegis Ridge. The D.S.D.P. Site 402 heat flux determination was located slightly higher on the slope (figure 3).

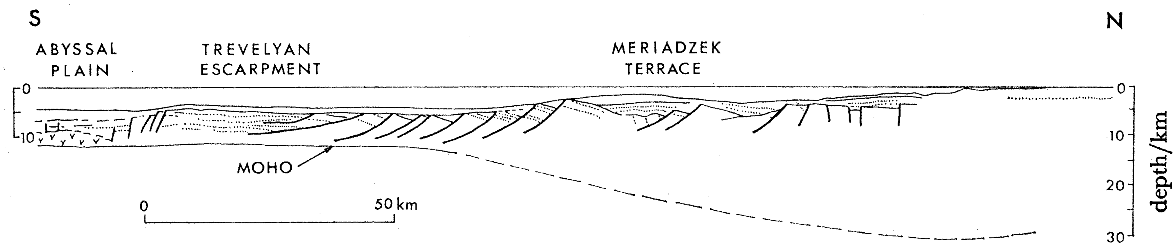

FIGURE 2. Cross section of the Western Approaches continental margin along seismic reflexion profile OC 209 after Montadert *et al.* (1979). Location of profile in figure 1.

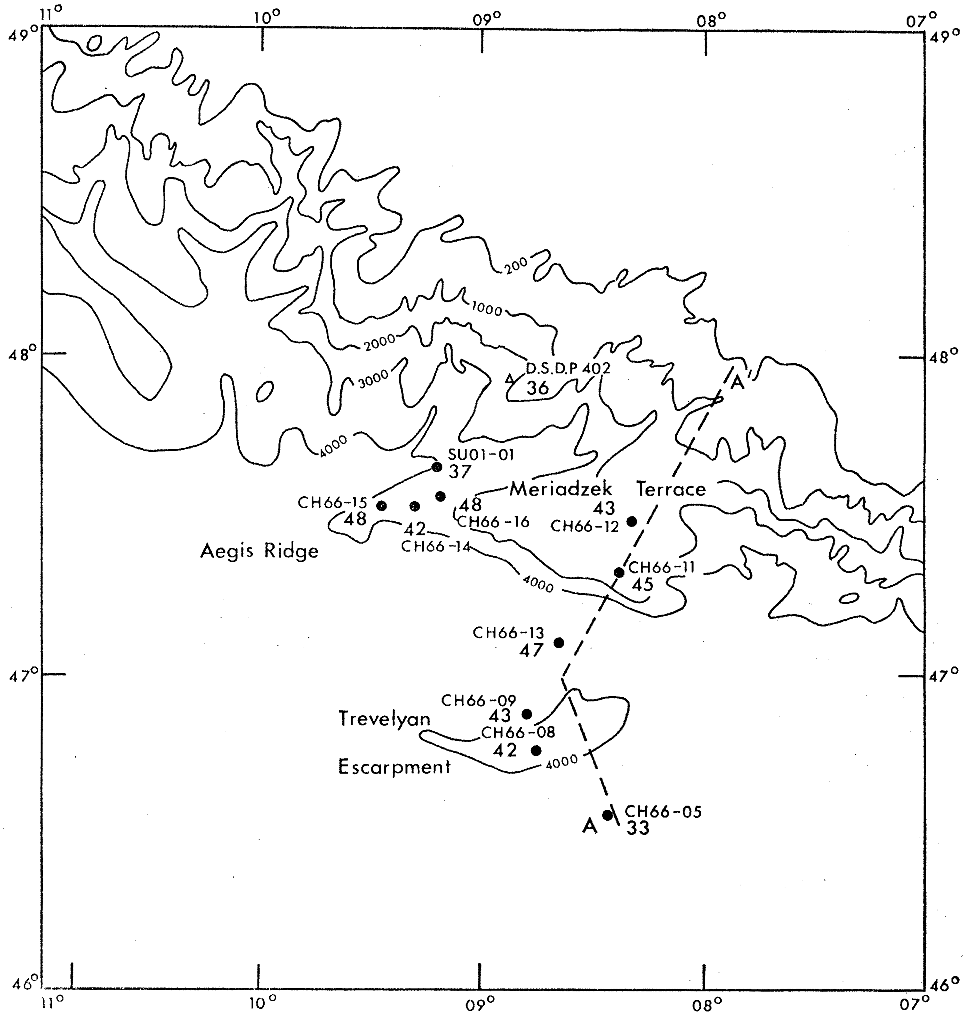

FIGURE 3. Location map of the C.N.E.X.O. heat flow measurements over the Western Approaches continental margin. The D.S.D.P. Site 402 heat flow determination is shown by a triangle. The heat flow values are in mW m^{-2}.

Surface geothermal data

The temperature gradients were determined from the temperatures measured at up to five different depths in the upper 2–10 m of sediment by means of thermistor temperature probes attached at known vertical distances along the 10 m long barrel of a piston corer (Gerard *et al.* 1962). At each site, the temperature of each probe was measured about every 10 s for a total period of about 6 min, during which the corer was left undisturbed in the sediment. The recording device, of the Wheatstone bridge and film recording (Lamont) type described by Langseth (1965), was housed in a pressure vessel at the top of the corer. Equilibrium temperatures in the sediment were extrapolated from the temperature transients recorded, by linear fitting of the temperatures against the reciprocal of time (Bullard 1954). The accuracy of the temperatures determined in the sediment with respect to the bottom water temperature is better than 0.005 °C.

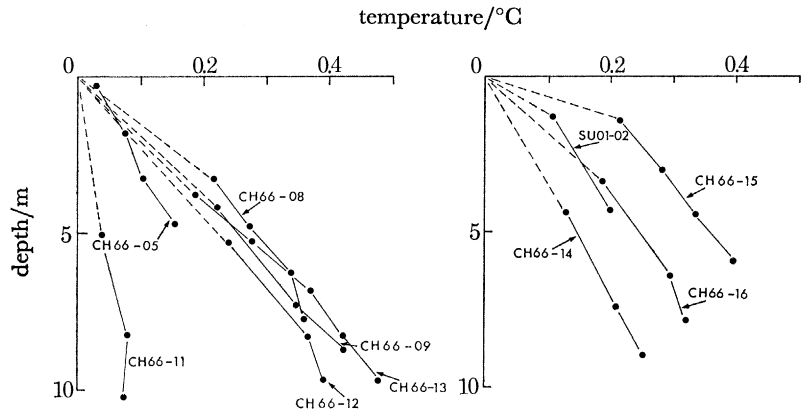

Figure 4 Figure 5

Figure 4. Temperature profiles in sediment at stations located along profile AA′ (figure 3). Note the anomalously low gradient at station CH 66–11. Temperatures are relative to the bottom water temperature at each station.

Figure 5. Temperature profiles in sediment for the four stations over the Aegis Ridge. Temperatures are relative to the bottom water temperature at each station.

The thermal conductivity of the sediment was measured on board the ship at several points along each core recovered, in most cases every 50 cm, by using the transient needle probe technique (Von Herzen & Maxwell 1959) and correcting the values to *in situ* temperature and pressure conditions (Ratcliffe 1960). The accuracy of the needle probe technique has been estimated to 3–4 % (Von Herzen & Maxwell 1959). Larger errors can, however, occasionally occur, owing to mechanical disturbances of the sediment either during the coring operation itself or afterwards during handling the core on board the ship. In practice, conductivity values departing significantly from the trend defined by the other values were eliminated in the absence of notable apparent changes in the lithology of the sediment.

The temperature profiles in the sediment are linear to a first approximation (figures 4 and 5). The linearity is in particular indicated by the agreement between the extrapolated surface sediment temperatures and the measured bottom water temperatures (table 1). Pronounced curvatures downwards were, however, observed at station CH 66–08 over Trevelyan (figure 4) and stations CH 66–14, CH 66–15 and CH 66–16 over the Aegis ridge (figure 5). Bottom water temperature fluctuations may be one possible explanation of the curvature (see, for example, Pugh 1975) but, in the absence of available long-term bottom-water temperature records, this explanation remains hypothetical. However, at station CH 66–15 where the maximum difference between the extrapolated and measured bottom water temperatures occurs, the four temperature points at depths in the sub-bottom between 1.5 and 5.9 m are nearly perfectly aligned. If the curvature of the temperature profile at station CH 66–15 results from bottom water temperature fluctuations, the shape of the temperature profile then suggests that these fluctuations are of short periods (periods of a few days or weeks) penetrating only to small depths in the sediment (Pugh 1975). The occurrence of short-term bottom-water temperature fluctuations may be related to instability of the water masses along the slope of the margin. In the absence of any evidence on which to rely on to apply corrections to the observed temperature profiles, no correction has been made. We consider the stations where pronounced curvature of the temperature profiles are observed as being of moderate quality.

Table 1 summarizes the data obtained. The heat flux value at each station is simply taken as the product of the mean vertical temperature gradient and the mean harmonic thermal conductivity. The corrected heat flux values include corrections applied to account for the

Table 1. Summary of the C.N.E.X.O. heat flow measurements over the Western Approaches margin

(Included is the D.S.D.P. site 402 heat flow determination (Erickson *et al.* 1979.)

station	position latitude N	longitude W	water depth/m	bottom water temperature °C	penetration/m	no. of temp. in sed.
SU01–01	47° 39.6′	9° 13.8′	3826	2.52	4.3	2
CH66–05	46° 32.5′	8° 26.5′	4732	2.54	4.7	4
CH66–08	46° 44.5′	8° 44.9′	3641	2.58	7.7	4
CH66–09	46° 51.5′	8° 48.7′	4081	2.53	8.7	3
CH66–11	47° 18.1′	8° 23.1′	2789	2.89	10.2	3
CH66–12	47° 28.3	8° 19.3′	2095	3.52	9.7	3
CH66–13	47° 05.8′	8° 40.9′	4378	2.52	9.7	5
CH66–14	47° 31.3′	9° 19.9′	3304	2.65	8.8	3
CH66–15	47° 32.0′	9° 28.6′	4052	2.52	5.9	4
CH66–16	47° 33.5′	9° 12.2′	2972	2.83	7.7	3
Ipod Site 402	47° 52.5′	8° 50.4′	2339	3.40		

station	temperature gradient/km^{-1} (b.w.t. extrapolated)	no. of conductivity measurements	thermal conductivity/ W m^{-1} K^{-1}	heat flow/mW m^{-2}	topographical correction (%)	sediment correction (%)	corrected heat flow/ mW m^{-2}
SU01–01	30 (2.59)	7	1.22 ± 0.18	37	−5	5	37
CH66–05	28 (2.56)	4	1.17 ± 0.05	33	−4	5	33
CH66–08	34 (2.69)	13	1.09 ± 0.07	37	7	5	42
CH66–09	38 (2.60)	19	1.05 ± 0.10	40	4	5	43
CH66–11	< 13 (2.90)	15	1.09 ± 0.04	< 14	0	5	< 15
CH66–12	32 (3.60)	12	1.25 ± 0.16	40	4	5	43
CH66–13	47 (2.55)	11	1.06 ± 0.04	50	−11	5	47
CH66–14	28 (2.63)	7	1.31 ± 0.05	37	10	5	42
CH66–15	40 (2.68)	6	1.14 ± 0.10	46	0	5	48
CH66–16	31 (2.90)	12	1.35 ± 0.23	42	10	5	48
Ipod Site 402	28.5		1.26 ± 0.07	36			

effects upon the near-surface temperature gradients of the large-scale topographic variations across the margin (topographic corrections in table 1) and of the sedimentation (sedimentary corrections in table 1). Topographic corrections were computed by solving the two dimensional steady state heat conduction equation (Sclater & Miller 1970) applied to topographic profiles across the margin (see, for example, figure 6). Topographic corrections are typically 5 %, with a maximum of 11 % at station CH 66–13 at the top of the Aegis Ridge. Sedimentary corrections

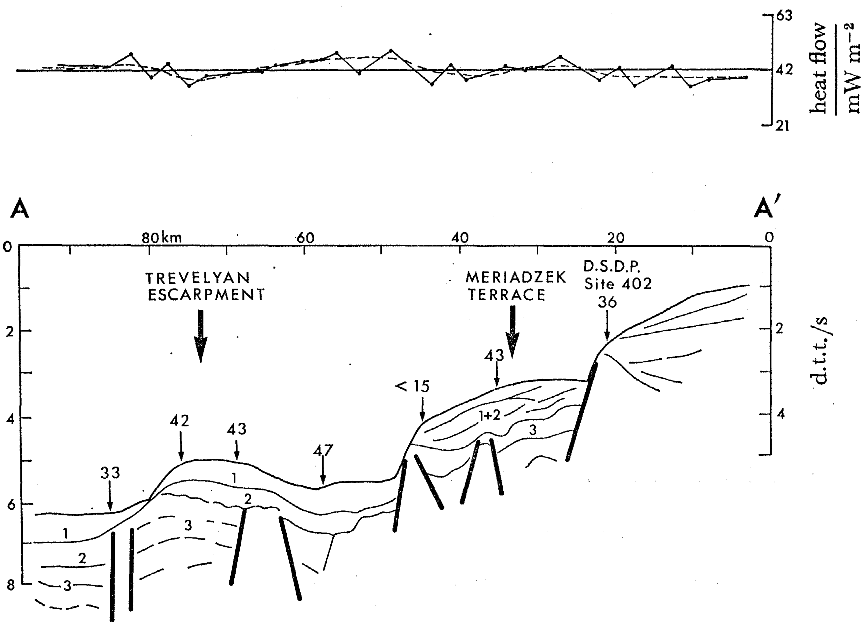

FIGURE 6. (Bottom.) Corrected heat flow measurements superimposed on the interpretated seismic profile AA′ from Montadert *et al.* (1974) located in figure 3. Sedimentary units as follows: (1) post-Eocene; (2) Cainomanian to Eocene; (3) Aptian–Albian. (Top.) Effects of the topography on the surface heat flux assuming a constant heat flux at depth of 42 mW m^{-2}. The dotted line is a smoothed curve.

were calculated by using the Von Herzen & Uyeda (1963) procedure, adopting a thermal diffusivity value of 3×10^{-3} cm^2 s^{-1} (Von Herzen & Maxwell 1959). For a total sedimentary thickness of 1–2 km, assumed to have been deposited at a uniform rate over the Meriadzek Trevelyan area since the end of rifting (110 Ma), the correction amounts to 3.3–6.6 %. Over the Aegis Ridge, sediments are lacking or reduced for the period ranging from 110–60 Ma. Assuming then that the *ca.* 1 km thick sediments have been deposited over the last 60 Ma, the correction amounts to 4.5 %. A 5 % average correction was applied to all measurements (table 1). The total correction at each station does not exceed 15 %, which justifies the simple correction procedures adopted above. The uncertainty on the corrected heat flux values is estimated to ± 20 %

RESULTS

Excluding station CH 66–11, where we have measured an abnormally low conductive heat flux, the mean conductive heat flux value calculated for the nine other stations is 43 ± 5 (s.d.) mW m^{-2}. There is no apparent trend in the heat flow distribution across the margin, with the exception, however, of a slightly lower value of 33 mW m^{-2} at station CH 66–05 at the foot of the Trevelyan Escarpment, in close proximity of the oceanic crust, which requires confirmation by further measurements. The surface heat flux data are in good agreement with the heat flow determination of 36 ± 14 mW m^{-2} reported for the D.S.D.P. Site 402 located slightly higher on the slope (Erickson *et al.* 1979). The thermal régime of the Western Approaches continental slope and rise appears then to be characterized by a low and fairly uniform regional heat flux of the order of 36–43 mW m^{-2}. The exceptionally low conductive heat flux measured at station CH 66–11 may indicate that conduction is not the dominant heat transfer process in the vicinity of this station. One may therefore suggest the occurrence of convective heat transfer along faults at the edge of the Meriadzek Terrace.

Comparison with heat flux data of the adjacent continental and oceanic areas

Figure 7 shows the compilation of the available heat flux data in Western Europe and the Bay of Biscay. Included are the surface heat flow data obtained over the Western Approaches margin reported here and the heat flow determinations at D.S.D.P. Site 402 (Erickson *et al.* 1979). The compilation is based on the world heat flow data compilation by Jessop *et al.* (1976) and for data in France on recent compilations made by Gable (1977) and Bertaux *et al.* (1978). The background heat flux in France over stable portions of the Hercynian continental crust is of the order of 65–85 mW m^{-2}. This range of values is comparable with the 72.5 ± 19.8 (s.d.) mW m^{-2} heat flux average calculated for the Hercynian fold belt in Central Europe from a total of 147 measurements (Hurtig & Oelsner 1977). In southwest England, a similar value of 67 mW m^{-2} was obtained, while the two other exceptionally high values, of 134 and 137 mW m^{-2}, are thought to be due partly to a high crustal radioactivity associated with the Cornwall batholith and partly to hydrothermal effects (Tammemagi & Wheildon 1974). Compared to the background heat flux in Western Europe, the heat flux over the Western Approaches margin then appears to be reduced by a factor of nearly two. In contrast, heat flow values over the margin are similar to those in the Bay of Biscay. The average of the five available heat flux values in the Bay of Biscay is 45 ± 10 (s.d.) mW m^{-2}.

Implications

We note first that the elapsed time since the last major thermal event to have affected the Western Approaches margin (dated at 100 Ma, corresponding to the end of rifting before the onset of opening of the Bay of Biscay in Upper Aptian), is considerably more than the thermal time constant of the lithosphere, i.e. a few tens of millions of years. This implies that the Western Approaches margin is close to thermal equilibrium. This is true *a fortiori* for the stable Hercynian continental area where the time since the last major thermal event to have affected the lithosphere (*ca.* 280 Ma) is still larger. Nearly steady state thermal conditions therefore characterize the thermal regime of both the Western Approaches margin and the adjacent Western European continental area. The steady state surface heat flow Q_s can be seen as the sum of two components, the crustal radioactive heat production Q_c and the heat flux from the mantle Q_m. If one neglects the lithospheric mantle radioactive heat production, which is unlikely to exceed a few mW m^{-2} (see, for example, Bickle 1978) the mantle heat flux is, to a first approximation, the heat flux at the base of lithosphere. Consequently, the heat flux contrast observed between the Western Approaches margin and the adjacent stable Hercynian Western European continental

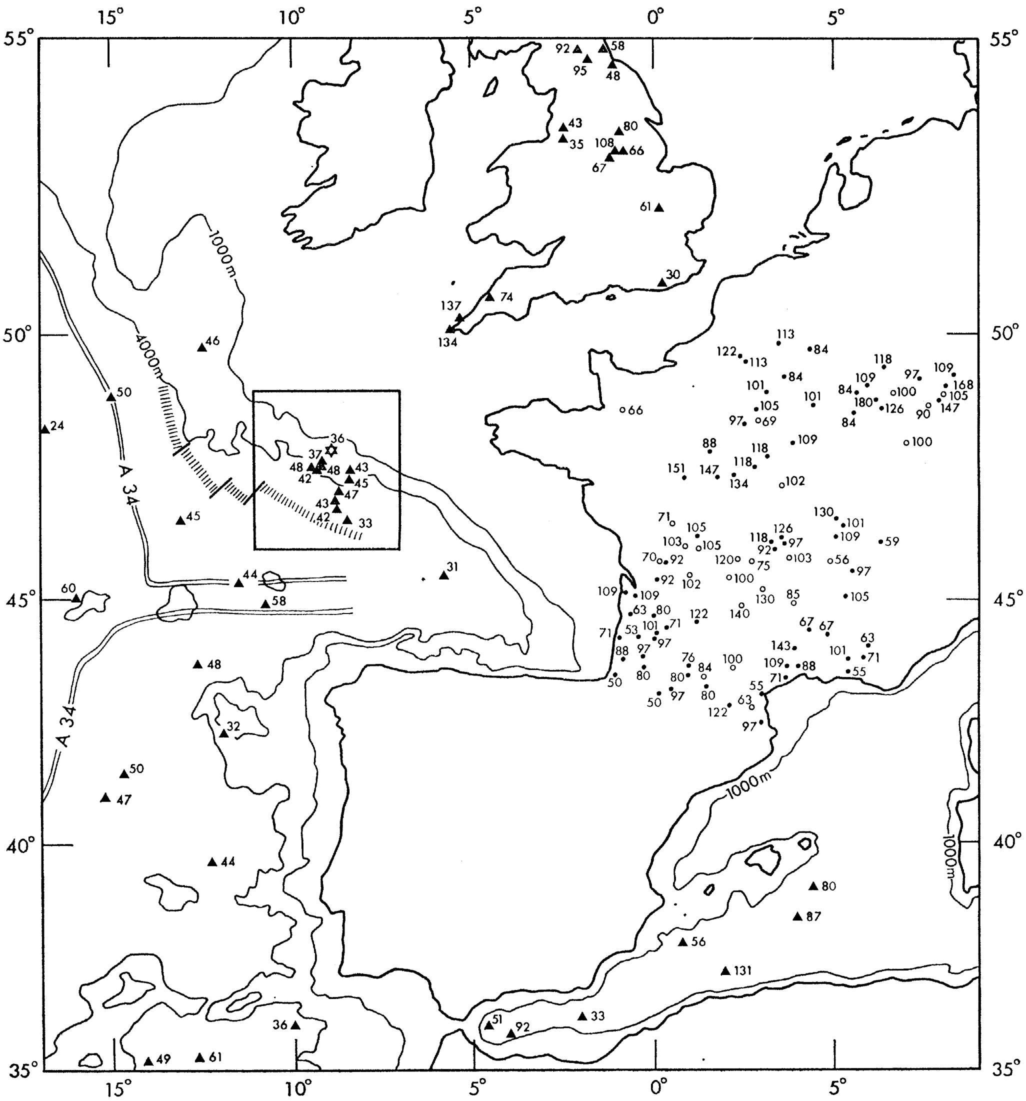

Figure 7. Compilation map of the available heat flow data in Western Europe and the Bay of Biscay. Sources: Jessop *et al.* (1976) (triangles); Gable (1977) (full circles); Bertaux *et al.* (1978) (open circles); Erickson *et al.* (1979) (star); this study (triangles in the box). The hatched area shows the continental–oceanic crust boundary.

Table 2. Estimates of the surface heat flow Q_s, the crustal contribution Q_c and the mantle heat flux Q_m for the Western Approaches continental slope and rise and the adjacent oceanic and continental areas

(The 25 mW m^{-2} Q_m value given for the Bay of Biscay is a mean estimate for the oceanic regions (Kono & Yoshii 1975).)

	Bay of Biscay oceanic crust	Western Approaches continental slope	West European Hercynian continental crust
age of last thermal event/Ma	70–110	110	280
Q_s/(mW m^{-2})	35–55	36–43	65–85
Q_m/(mW m^{-2})	(25)	24–30	24–30
Q_c/(mW m^{-2})	(10–30)	6–19	35–61
$Q_c(L)/Q_c(L_0)$	—	0.11–0.46	

area can be explained in terms of either different crustal contributions or different heat flux at the base of the lithosphere or even a combination of these two causes. Since both the Western Approaches margin and the adjacent continent belong to one same stable portion of the European plate, we see *a priori* no reason why the heat flux at the base of the lithosphere would vary from one area to the other, so that the second explanation appears to be less likely. We therefore suggest that the observed heat flux contrast reflects different crustal contributions.

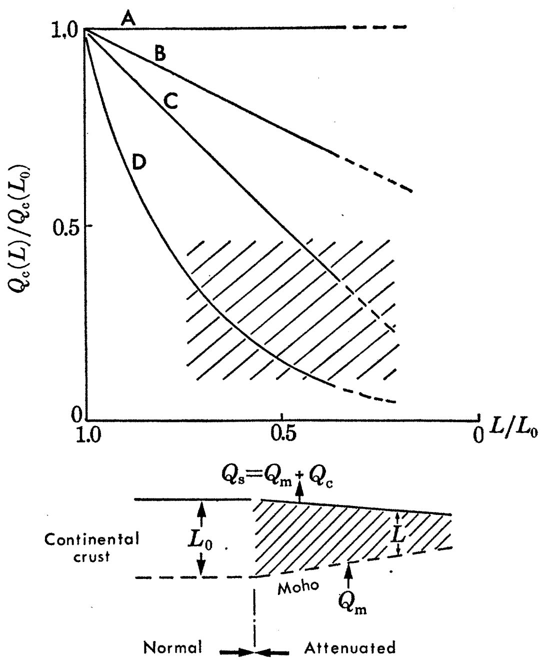

FIGURE 8. Predicted change in the crustal contribution to the surface heat flow assuming various mechanisms of crustal thinning. (A) Deep crustal metamorphism (Falvey 1974; Ringwood & Green 1966; Colette 1968). (B) Creep in lower crust (Artemjev & Artyushkov 1971; Bott & Dean 1972). (C) Crustal stretching (Artemjev & Artyushkov 1971; Morton & Black 1975). (D) Surface erosion (Sleep 1971). Q_c and Q_m are respectively the crustal and mantle contributions to the surface heat flow Q_s. L_0 and L are thicknesses of respectively the normal and thinned continental crust. The hatched area gives the window corresponding to the heat flow constraints (see text).

Table 2 illustrates our approach in providing tentative estimates of the crustal contributions Q_c and the mantle heat flux Q_m for the Western Approaches margin and the adjacent continental and oceanic areas. The 24–30 mW m^{-2} Q_m value used for Western Europe, also adopted for the Western Approaches margin, is the estimate derived by Daignères & Vasseur (1979) for the Bournac site in the Central Massif in France. At this site, the measured surface heat flow is 85 mW m^{-2}, so that about two thirds of the surface heat flux would be accounted for by crustal radioactivity. Based on the 24–30 mW m^{-2} Q_m value derived at the Bournac site, which is to our knowledge the only Q_m estimate available in Western Europe, the crustal contribution for the Western Approaches margin would therefore be only a fraction composed of between 0.11 and 0.46 of the crustal contribution for Western Europe (table 2). Allowing for some uncertainty in the Q_m value, since the regional validity of the Bournac site estimate may be questioned, a higher Q_m value would still increase the amount of reduction of the crustal contribution, while an upper limit of the possible amount of reduction is given by the case of the mantle heat flux taken equal to zero; $Q_c(L)/Q_c(L_0)$ would be then equal to $Q_s(L)/Q_s(L_0)$ and would occur between 0.42 and 0.66.

If the above approach is correct, one important implication of the heat flow results is to require crustal thinning processes under the margin capable of producing a large reduction of the crustal radioactive heat production. Figure 8 illustrates schematically the possibility of four main types of crustal thinning to decrease the crustal radioactive heat production. One fundamental preliminary observation is then that if crustal thinning reflects only an upward migration of the Moho as a result of deep metamorphic changes such as gabbro to eclogite (Ringwood & Green 1966; Colette 1968) or Greenshist to amphibolite (Falvey 1974), no variation is expected in the steady state surface heat flux in so far as each lithospheric column can be considered as a closed system for the radiogenic sources contained in this column, which is assumed here (figure 8, curve A). In other words, we assume that there is no lateral migration of the radiogenic sources and no input of new radiogenic sources from below. Applied to the Western Approaches margin, this means that deep metamorphism processes are unlikely to be the dominant cause of the crustal thinning since these processes would not account for the large reduction of the surface heat flow. In contrast to deep metamorphism, the three other processes considered in figure 8 can produce a significant decrease of the crustal radioactive contribution. One of these processes is surface erosion, generally related to doming of the continental crust in the early stage of formation of a rifted margin (Closs 1939; Sleep 1971). If radiogenic sources are mainly concentrated in the upper crustal material, as generally believed (see, for example, Roy *et al.* 1968; Lachenbruch 1968), surface erosion is expected to cause a rapid decrease of the crustal contribution since it would remove the more radiogenic crustal material (figure 8, curve B). However, the loss of radiogenic sources during erosion can be compensated to some extent by the radioactive contribution of the sediments deposited after erosion. The two other processes considered in figure 8 involve a purely mechanical deformation of the crust under tensional forces developed either during rifting (Artemjev & Artjuskyov 1971; Morton & Black 1975) or in the early stage of opening of a new ocean, in this latter case as a result of unequal loading and associated isostatic compensation across the margin (Bott 1971; Bott & Dean 1972). The extension would then occur through brittle faulting of the upper crust and ductile deformation of the lower crust. If the amount of extension is, to a first approximation, constant with depth through the whole thickness of the crust, the crustal radioactive contribution would decrease linearly with the amount of crustal thinning, whatever the radiogenic sources distribution model adopted (figure 8, curve C). If the extension affects mainly the deep crust (Bott 1971; Bott & Dean 1972), the decrease in the crustal radioactive contribution is difficult to assess since it depends largely on the crustal deformation and radiogenic source distribution models adopted, but in any case would be less than for the case of a uniform extension of the crust (figure 8, curve D).

Surface erosion must be eliminated as a possible process of crustal thinning under the Western Approaches margin, since there is evidence that no erosion occurred before and during rifting in the central trough of the rift system (Montadert *et al.* 1979). Then, one possible explanation of the large reduction of the surface heat flux is to presume that the dominant process of crustal thinning under the margin was crustal extension. In this respect, assuming that the one half reduction of the crustal thickness under the continental slope and rise of the Western Approaches margin is a result of a purely extensive deformation uniformly affecting the whole thickness of the crust, the predicted change in the crustal contribution Q_c is a reduction also of about one half (applying curve C in figure 8), which is within the range of the estimated reduction values in table 2. Such a large extension of the original continental crust suggested by the interpretation above is much more than the 15% extension estimated by Montadert *et al.* (1979) from a reconstruction of the displacements of the tilted fault blocks along fault planes.

We thank J. Francheteau for a critical reading of the manuscript, D. Roberts and L. Montadert for their encouragement, and D. Carré and Y. Potard for technical assistance.

References (Foucher & Sibuet)

Artemjev, M. E. & Artjuskyov, E. V. 1971 *J. geophys. Res.* **76**, 1197–1211.
Auffret, G. A., Pastouret, L., Cassat G., De Charpal, O., Cravatte, J. & Guennoc, P. 1979 In *Init. Rep. D.S.D.P.* vol. 48 (in the press).
Avedik, F. & Howard, D. 1979 In *Init. Rep. D.S.D.P.* vol. 48 (in the press).
Bertaux, M. G., Bienfait, G., Bottinga, Y., Fontaine, J., Guyot, G., Jolivet, J., Kast, Y., Meunier, J., Ottlé, J., Perrier, G., Poupinet, G. & Vasseur, G. 1978 *C. r. hebd. Séanc. Acad. Sci., Paris* **286**, 933–936.
Bickle, M. J. 1978 *Earth planet. Sci. Lett.* **40**, 301–315.
Bott, M. H. P. 1971 *Tectonophysics*, **11**, 319–327.
Bott, M. H. P. & Dean, D. S. 1972 *Nature, Lond.* **235**, 23–25.
Bullard, E. C. 1954 *Proc. R. Soc. Lond.* A **222**, 408–429.
Closs, H. 1939 *Geol. Rdsch.* **30**, 405–527.
Colette, B. J. 1968 In *Geology of shelf areas* (ed. Donavan), pp. 15–30. Edinburgh: Oliver & Boyd.
Daignères, M. & Vasseur, G. 1979 *Ann. Géophys.* **35**, 1–9.
Erickson, A. J., Avera, W. E. & Byrne, R. 1979 In *Init. Rep. D.S.D.P.* vol. 48 (in the press).
Falvey, D. A. 1974 *Aust. Petrol. Exploration Ass.* **14**, 95–106.
Gable, R. 1977 *Edn. Bur. Rech. géol. miner., Paris* 121–122.
Gerard, R., Langseth, M. G. & Ewing, M. 1962 *J. geophys. Res.* **67**, 785–803.
Hurtig, E. & Oelsner, C. 1977 *Tectonophysics* **41**, 147–156.
Jessop, A. M., Hobart, M. A. & Sclater, J. G. 1976 *The world heat flow data collection* 1975. Geothermal service of Canada; Energy, Mines and Resources Canada, Earth Physics Branch, Ottawa, vol. 5, pp. 1–125.
Kono, Y. & Yoshii, J. 1975 *J. phys. Earth* **23**, 63–75.
Lachenbruch, A. H. 1968 *J. geophys. Res.* **73**, 6977–6989.
Langseth, M. G. 1965 In *Terrestrial heat flow* (ed. W. H. K. Lee), vol. 8, pp. 58–77. Geophysical Monograph series, American Geophysical Union.
Montadert, L., Winnock, E., Delteil, J. R. & Grau, G. 1974 In *The geology of continental Margins* (ed. C. A. Burk & C. L. Drake), pp. 323–342. New York: Springer–Verlag.
Montadert, L., De Charpal, O., Roberts, D., Guennoc, P. & Sibuet, J. C. 1979 In *M. Ewing Symposium II proceedings* (in the press).
Morton, W. H. & Black, R. 1975 In *Afar Depression of Ethiopia* (ed. Pilger & Rösler) vol. 1, pp. 55–65. Stuttgart: Schweizerbart'sche Verlagsbuchlandlung.
Pautot, G., Renard, V., Auffret, G. A., Pastouret, L. & De Charpal, O. 1976 *Nature, Lond.* **263**, 669–672.
Pugh, D. T. 1975 *Earth and planet. Sci. Lett.* **27**, 121–126.
Ratcliffe, E. H. 1960 *J. geophys. Res.* **65**, 1535–1541.
Ringwood, A. E. & Green, D. H. 1966 *Tectonophysics* **3**, 383–427.
Roy, R. F., Blackwell, D. D. & Birch, F. 1968 *Earth planet. Sci. Lett.* **5**, 1–12.
Sclater, J. G. & Miller, S. P. 1970 *Tectonophysics* **10**, 283–300.
Sleep, N. H. 1971 *Geophys. J. R. Astr. Soc.* **24**, 325–350.
Tammemagi, H. Y. & Wheildon, J. 1974 *Geophys. J. R. Astr. Soc.* **38**, 83–94.
Von Herzen, R. P. & Uyeda, S. 1963 *J. geophys. Res.* **68**, 4219–4250.
Von Herzen, R. & Maxwell, A. E. 1959 *J. geophys. Res.* **64**, 1557–1563.

PHILOSOPHICAL TRANSACTIONS OF THE ROYAL SOCIETY A MATHEMATICAL, PHYSICAL & ENGINEERING SCIENCES